Is the GFR-based scaling approach adequate for predicting pediatric renal clearance of drugs with passive tubular reabsorption? Insights from PBPK modeling

Sanwang Li[1,2,3] | **Xuexin Ye**[1] | **Qiushi Wang**[1] | **Zeneng Cheng**[1] |
Feiyan Liu[1] | **Feifan Xie**[1]

[1]Division of Biopharmaceutics and Pharmacokinetics, Xiangya School of Pharmaceutical Sciences, Central South University, Changsha, China

[2]Department of Pharmacy, The Second Xiangya Hospital, Central South University, Changsha, China

[3]Institute of Clinical Pharmacy, Central South University, Changsha, China

Correspondence
Feifan Xie, Xiangya School of Pharmaceutical Sciences, Central South University, Tongzipo road 172, Changsha 410013, China.
Email: feifan.xie@csu.edu.cn

Abstract

Empirical maturation models (e.g., Johnson and Rhodin models) for glomerular filtration rate (GFR) are commonly used as scaling factors for predicting pediatric renal clearance, but their predictive performance for drugs featured with tubular reabsorption is poorly understood. This study investigated the adequacy of GFR-based scaling models for predicting pediatric renal clearance in drugs with passive tubular reabsorption by comparing with a mechanistic kidney model (Mech-KiM) that encompasses the physiological processes of glomerular filtration, tubular secretion, and reabsorption. The analysis utilized hypothetical drugs with varying fractions of tubular reabsorption (F_{reabs}), alongside the model drug metronidazole, which has a F_{reabs} of 96%. Our simulations showed that when F_{reabs} is ≤70%, the discrepancies between the GFR-based scaling methods and the Mech-KiM model in predicting pediatric renal clearance were generally within a twofold range throughout childhood. However, for drugs with substantial tubular reabsorption (e.g., $F_{reabs} > 70\%$), discrepancies greater than twofold were observed between the GFR-based scaling methods and the Mech-KiM model in predicting renal clearance for young children. In neonates, the differences ranged from 5- to 10-fold when the adult F_{reabs} was 95%. Pediatric physiologically based pharmacokinetic (PBPK) modeling of metronidazole revealed that using a GFR-based scaling method (Johnson model) significantly overestimated drug concentrations in children under 2 months, whereas utilizing the Mech-KiM model for renal clearance predictions yielded estimates closely aligned with observed concentrations. Our study demonstrates that using GFR-based scaling models to predict pediatric renal clearance might be inadequate for drugs with extensive passive tubular reabsorption (e.g., $F_{reabs} > 70\%$).

Sanwang Li and Xuexin Ye contributed equally.

Study Highlights

WHAT IS THE CURRENT KNOWLEDGE ON THE TOPIC?

Empirical maturation models, such as the Johnson and Rhodin models, are commonly employed as scaling factors to predict pediatric renal clearance, while a mechanistic kidney model (Mech-KiM) has also been proposed and applied successfully to predict pediatric renal clearance by incorporating the physiological processes of renal excretion in an age-dependent manner.

WHAT QUESTION DID THIS STUDY ADDRESS?

It remains unclear whether GFR-based scaling models are adequate to predict pediatric renal clearance for drugs that undergo tubular reabsorption. We investigated the predictive performance of GFR-based scaling models by comparing to the Mech-KiM model using a physiologically-based pharmacokinetic (PBPK) modeling and simulation approach, utilizing hypothetical drugs with various degrees of passive tubular reabsorption and a model drug metronidazole with a fractional tubular reabsorption (F_{reabs}) of 96%.

WHAT DOES THIS STUDY ADD TO OUR KNOWLEDGE?

GFR-based scaling methods are adequate for predicting pediatric renal clearance for drugs with a $F_{\text{reabs}} \leq 70\%$, whereas the Mech-KiM model might be considered for drugs with a $F_{\text{reabs}} > 70\%$.

HOW MIGHT THIS CHANGE DRUG DISCOVERY, DEVELOPMENT, AND/OR THERAPEUTICS?

The analysis conducted in this study provides valuable insights into prediction of pediatric renal clearance of drugs with passive tubular reabsorption. This is beneficial for using PBPK modeling for pharmacokinetic predictions and dose optimization in children.

INTRODUCTION

Renal elimination is a primary pathway for the excretion of a wide range of drugs (e.g., angiotensin converting enzyme inhibitors, beta-lactams, and antineoplastics).[1–3] Glomerular filtration, tubular secretion, and tubular reabsorption are the fundamental processes determining the rate of urinary excretion of a drug.[4] Glomerular filtration is a passive process driven by hydrostatic pressure. Tubular secretion is a mechanism involving carriers that transport drug molecules from the blood into the proximal tubule. Tubular reabsorption is mostly passive, particularly for exogenous drugs (e.g., linezolid, moxifloxacin, and metronidazole).[5,6] Additionally, pinocytosis is an important mechanism of renal tubular reabsorption for large molecules, such as proteins.

Prediction of renal clearance (CL_R) of a drug in children is a key component in understanding the developmental pharmacokinetics (PK) of a drug. Physiologically based pharmacokinetic (PBPK) modeling is a useful tool for predicting the drug exposure levels in pediatrics at different ages by incorporating age-specific physiological parameters such as organ sizes, blood flows, metabolic enzyme activities, and other variables (e.g., renal function)

that alter with growth and development.[7,8] In PBPK modeling, age-dependent renal clearance in pediatrics is typically scaled from adult values based on changes in glomerular filtration rate (GFR). Various maturation models, such as the widely used Johnson and Rhodin models,[9,10] have been developed to describe age-related changes in GFR in entire pediatric populations. The Johnson and Rhodin models are developed based on the renal clearance of exogenous markers (e.g., mannitol, iohexol, inulin, and ^{51}Cr-EDTA) with simply glomerular filtration,[11,12] making them most suitable for drugs excreted renally via glomerular filtration.

Using GFR as a scaling factor for pediatric renal clearance implies that tubular secretion and reabsorption have the same maturation characteristics as glomerular filtration.[13] However, glomerular filtration, tubular secretion, and reabsorption exhibit independent patterns of development.[6] The GFR matures more quickly than passive tubular secretion, leading to a glomerulo-tubular imbalance in neonates, while passive tubular reabsorption is the final renal function to develop.[11] Therefore, these renal processes should ideally be considered separately to accurately account for their contributions to drug's renal excretion in children. It is well-recognized that the empirical

GFR approach is unsuitable for scaling renal clearance of drugs with significant tubular secretion in young children, especially infants, because the ontogeny profiles of renal transporters (e.g., organic anion transporters [OATs] 1 and 3) for tubular secretion differ from that of GFR.[14] Unlike active renal secretion, renal tubular reabsorption is typically a passive process, similar to glomerular filtration. Currently, the empirical GFR scaling approach is usually the first choice for predicting pediatric renal clearance for drugs with tubular reabsorption. This method assumes a fixed fractional tubular reabsorption for these drugs between adults and children,[15] thereby neglecting the maturation process of tubular reabsorption. Unfortunately, the predictive performance of GFR-based scaling models for predicting pediatric renal clearance of drugs with tubular reabsorption has not been investigated, leaving it unclear whether this approach is adequate for such drugs.

In recent years, a mechanistic kidney (Mech-Kim) model has been developed for the prediction of renal elimination in adults and pediatrics.[13,16] In this physiological model, the nephron consists of eight segments: the glomerulus, followed by three segments of the proximal tubule, the Loop of Henle, the distal tubule, and collecting ducts (cortex and medulla segments). Each segment comprises three compartments: tubular fluid, cell mass, and blood space. Drug movement between compartments and segments is described by ordinary differential equations that maintain mass balance (Figure S1). The Mech-Kim model allows the quantitative description of the physiological parameters (e.g., GFR and urine flow rate) for the processes of glomerular filtration, tubular secretion, and reabsorption in an age-dependent manner. This makes it a feasible method for predicting pediatric renal clearance for drugs involving any of these processes individually or in combination. The use of the Mech-KiM model has proven to provide accurate predictions for drugs (e.g., cimetidine, ciprofloxacin, metformin, tenofovir, and zidovudine) with tubular secretion in children aged 1 day to 18 years.[13] Theoretically, the Mech-KiM model is also suited for predicting pediatric renal clearance for drugs featured with tubular reabsorption.

This study aimed to evaluate the adequacy of GFR-based scaling methods in predicting pediatric renal clearance for hypothetical drugs with varying degrees of passive tubular reabsorption, using the Mech-KiM model as a reference. The predictive performance of pediatric pharmacokinetics by empirical and mechanistic methods was assessed using metronidazole as a model drug through a PBPK modeling approach.

MATERIALS AND METHODS

Prediction of pediatric renal clearance for hypothetical drug with tubular reabsorption

Hypothetical drug and pediatric characteristics

The hypothetical drug underwent both glomerular filtration and tubular reabsorption and bound to human serum albumin. In adults, the considered values of the fraction unbound (f_u) in plasma for this hypothetical drug were 0.9, 0.5, and 0.1, and various fractions of tubular reabsorption (F_{reabs}) were taken into account, with values of 10%, 30%, 50%, 70%, 80%, 90%, and 95%. The standard GFR in adults (GFR_{adult}) was assumed to be 120 mL/min. Based on the predefined values of F_{reabs}, f_u, and GFR_{adult}, the adult CL_R were back-calculated according to Equation 1.[6] The relationships of F_{reabs}, f_u, and adult CL_R are summarized in Table 1.

$$F_{reabs} = \left(1 - CL_R / \left(f_u \times GFR_{adult}\right)\right) \times 100\% \quad (1)$$

The Sim-Pediatric module in Simcyp simulator V22 was used to generate the typical demographics of the pediatric subgroups with different postnatal age (PNA). PNA

TABLE 1 The relationships of fractions of tubular reabsorption (F_{reabs}), fraction unbound in plasma (f_u), adult renal clearance (CL_R), and intrinsic passive diffusion clearance (CL_{PD}) of the virtual drug.

| F_{reabs} | $f_u = 0.9$ | | $f_u = 0.5$ | | $f_u = 0.1$ | |
	CL_R (L/h)	CL_{PD} (mL/min/ million cells)	CL_R (L/h)	CL_{PD} (mL/min/ million cells)	CL_R (L/h)	CL_{PD} (mL/min/ million cells)
10%	5.832	0.00045	3.240	0.00045	0.648	0.00045
30%	4.536	0.0010	2.520	0.0010	0.504	0.0010
50%	3.240	0.0020	1.800	0.0020	0.360	0.0020
70%	1.944	0.0042	1.080	0.0042	0.216	0.0042
80%	1.296	0.0060	0.720	0.0060	0.144	0.0060
90%	0.648	0.0160	0.360	0.0160	0.072	0.0160
95%	0.324	0.043	0.180	0.043	0.036	0.043

values for the pediatrics at 0.0027 (1 day), 0.0192 (7 days), 0.0411 (15 days), 0.0833 (1 month), 0.1667 (2 months), 0.5, 1.0, 2.0, 6.0, 12.0, and 18.0 years old were considered. The age and other generated demographics are shown in Table 2.

Empirical GFR-based scaling approach

The empirical Johnson and Rhodin models were assessed for predicting pediatric renal clearance of the hypothetical drug. The Johnson model was the default method in the Simcyp simulator for estimating GFR in pediatrics (from term neonates to adulthood) using the Sim-Pediatric module. This model employed body surface area (BSA, m^2) to predict GFR in pediatrics (Equation 2). Based on the BSA of the selected pediatrics, the estimated GFR using Johnson model is presented in Table 2. The Rhodin model described a nonlinear model using body weight (BW, kg) and postmenstrual age (PMA, weeks) to predict GFR from premature neonates to adulthood (Equation 3). The PMA was calculated as the sum of gestational age (GA) and PNA, and GA was assumed to be 40 weeks for the selected pediatrics in the Sim-Pediatric module. Based on the PMA and body weight of the selected pediatrics, the predicted GFR using the Rhodin model is shown in Table 2.

$$\text{GFR (mL / min)} = -6.1604 \cdot \text{BSA}^2 + 99.054 \cdot \text{BSA} - 17.74 \quad (2)$$

$$\text{GFR (mL / min)} = \left(\frac{\text{BW}}{70}\right)^{0.75} \cdot \left(\frac{\text{PMA}^{3.4}}{47.7^{3.4} + \text{PMA}^{3.4}}\right) \cdot 121 \quad (3)$$

The renal clearance of the hypothetical drug in pediatrics (CL$_{r,child}$) was scaled from the average value in adults (CL$_{r,adult}$) based on pediatric GFR (GFR$_{child}$) relative to adults (GFR$_{adult}$, with a standard value of 120 mL/min) using Equation 4.

$$\text{CL}_{r,child} = \frac{\text{GFR}_{child}}{\text{GFR}_{adult}} \cdot \text{CL}_{r,adult} \quad (4)$$

The age-dependent f_u of the hypothetical drug in children ($f_{u,child}$) was predicted using Simcyp and is listed in Table S1. The F_{reabs} of the hypothetical drug in children was then calculated based on Equation 1, using the predicted CL$_{r,child}$, GFR$_{child}$, and $f_{u,child}$.

Mech-Kim model

To enable the Mech-Kim model in Simcyp (Version 22) to predict pediatric renal clearance, the whole-body PBPK model should be utilized with additional drug input parameters. For this purpose, the above hypothetical drug was assigned with an arbitrary molecular weight of 300.0 g/mol, an arbitrary log$P$ of 1.0, and an arbitrary blood-to-plasma (B/P) concentration ratio of 1.0. The compound type of the drug was neutral. Tissue/plasma partition coefficients (K_p) were predicted using the Rodgers and Rowland method (Method 2 in Simcyp). The drug was assumed to be completely renally excreted, undergoing glomerular filtration and passive tubular reabsorption processes with the adult CL$_R$ values assigned as shown in Table 1. The Mech-Kim model accounts for passive tubular reabsorption across different regions of the nephron, with the majority occurring

TABLE 2 The demographics and predicted glomerular filtration rate (GFR) in pediatrics with different ages.

PNA (Years)	PMA (Weeks)	Body weight (kg)	Height (cm)	BSA (m^2)	Kidney weight (g)	Proximal tubule-segment 2 urine flow (mL/min)	Proximal tubule-segment 3 urine flow (mL/min)	GFR (mL/min, Johnson model)	GFR (mL/min, Rhodin model)
0.0027	40.14	3.03	52.71	0.21	22.34	2.72	2.25	3.01	4.11
0.0192	41.00	3.22	53.26	0.22	23.46	3.27	2.64	3.77	4.50
0.0411	42.14	3.47	53.99	0.23	24.90	4.00	3.18	4.74	5.04
0.0833	44.34	3.93	55.34	0.25	27.54	5.37	4.18	6.51	6.12
0.1667	48.69	4.79	57.90	0.28	32.29	7.84	5.97	9.65	8.37
0.5	66.07	7.60	66.58	0.38	46.94	15.49	11.52	19.14	17.20
1	92.14	10.48	76.03	0.48	60.90	23.31	17.20	28.20	26.32
2	144.29	13.63	87.46	0.58	75.31	30.86	22.68	37.81	34.66
6	352.86	20.82	116.13	0.82	106.11	47.59	34.83	59.34	48.68
12	665.71	37.05	148.27	1.25	169.15	77.39	56.46	96.50	75.07
18	978.57	69.80	177.64	1.87	282.43	103.67	75.54	134.74[a]	120.73

[a]For subjects older than 16 years, the units change to mL/min/1.73 m^2 to align with the default algorithm in Simcyp software. There was no urine flow in proximal tubule segment 1.

in the proximal tubule, smaller contributions from the distal tubule and Loop of Henle, and a negligible contribution from the collecting ducts. The bidirectional passive diffusion clearance (CL_{PD}, L/h) of the drug across the renal cell to the tubule and vice versa was assumed to be equal. The intrinsic CL_{PD} (mL/min/million cells) in both directions was the input parameter (Table 1) to calculate bidirectional CL_{PD} (L/h), combined with Proximal Tubular (PT) Cells per Gram of Kidney (PTCPGK, 99.4×10^6 cells per gram of kidney, unchanged with age) and kidney weight (KW, g) (Table 2), as shown in Equation 5. The maturation process of tubular reabsorption was characterized by the CL_{PD} parameter, with changes in CL_{PD} primarily driven by kidney weight in pediatric populations. With a specified adult virtual population (age range of 20 to 30 years and 100 male subjects), the intrinsic CL_{PD} parameter was manually adjusted to attain the desired simulated adult CL_R (Table 1). *The Sim-Pediatric module in* Simcyp were used for the hypothetical population simulations (10 trials with 10 subjects in each trial, male) for the pediatric subgroups with different postnatal ages (Table 2). A fixed intravenous single dose of 500 mg (arbitrary value) for the hypothetical drug was used across different pediatric ages. All the aforementioned parameters with assigned arbitrary values would impact the steady state volume of distribution. However, changes in these parameters did not influence the prediction of pediatric CL_R.

$$CL_{PD}(L/h) = CL_{PD}(mL/min/10^6 \text{ PT cells}) \times KW$$
$$\times PTCPGK \times 60 \times 10^{-3} \quad (5)$$

Age-related changes in GFR for the mechanistic kidney model in Simcyp were predicted using the implemented Johnson model for subjects up to 15 years old. For subjects older than 15 years, GFR was calculated using the Cockcroft and Gault equation.[13] The age-dependent urine flows in proximal tubule segments are presented in Table 2. In the Mech-Kim model, bladder urine flow is assumed to be 1 mL/min from childhood to adulthood due to insufficient physiological data. The F_{reabs} of the hypothetical drug in children, as predicted by the Mech-KiM model, was calculated using Equation 1, based on the predicted CL_R, f_u, and GFR in children.

To illustrate the impact of renal clearance predicted by the Mech-Kim model on overall drug clearance in pediatric populations, the hypothetical drug with an adult fraction unbound (f_u) of 0.5 (Table 1) was further analyzed by assuming varying ratios of renal clearance to total clearance in adults (0.1, 0.5, and 0.9), with non-renal elimination attributed to hepatic metabolism. Based on the calculated adult renal clearance in Table 1, the corresponding adult hepatic clearance was determined according to these assumed ratios. For the extrapolation from adults to children, no ontogeny of hepatic clearance was considered in order to simplify the scenario.

Case illustration of metronidazole

Metronidazole was chosen as a case illustration considering its pronounced tubular reabsorption (96%) and the availability of extensive clinical concentration data in both adults and pediatrics, which was valuable for verifying the PBPK model. In adults, metronidazole was primarily metabolized in the liver, with 94% of the dose undergoing metabolism. This process involved CYP2A6 (62% of the dose), CYP2E1 (22% of the dose), and UGT1A9 (10% of the dose).[17,18] The remaining 6% of the dose was eliminated through renal excretion. The dose fraction for each metabolic or excretion pathway was determined based on the mass balance in vivo study of metronidazole in healthy adults.[17,18] An adult intravenous PBPK model of metronidazole was initially developed using Simcyp (Version 22) and verified with clinical adult data. Subsequently, the adult PBPK model was scaled to pediatrics using the Sim-Pediatric module. In this process, both the empirical Johnson model (default in Simcyp) and the Mech-Kim model were employed to scale adult renal clearance to pediatrics. The predictive performance of the pediatric PBPK models using these two scaling approaches was evaluated with pediatric data at different ages.

Clinical data

The clinical concentration data of metronidazole administered intravenously in adults and pediatrics were obtained from literature through a PubMed search (up to March 8, 2024). Studies were included if (1) the subjects were healthy with no significant renal or hepatic impairment; (2) mean or individual-level concentrations were displayed in figures or tables in original studies; and (3) there was a clear description of study design elements (e.g., dosing regimens) and demographics (e.g., age).

A total of nine clinical studies on metronidazole were included for building the adult PBPK model (Table S2),[19–27] and three studies were enrolled for constructing the pediatric PBPK model (Table S3).[28–30] The concentration data were digitalized using the WebPlotDigitizer® software (version 4.8, https://apps.automeris.io/wpd4/).

Development of adult PBPK model

The adult PBPK model for metronidazole was constructed using the whole-body PBPK distribution model

embedded in Simcyp. The physicochemical parameters (such as $\log P$ and pK_a), drug f_u in plasma, and blood-to-plasma (B/P) ratio of metronidazole were all obtained from experimental measurements found in relevant literature (Table 3).[31–33] Tissue/plasma partition coefficients of metronidazole were predicted using the Rodgers and Rowland method in Simcyp and were further utilized to calculate the steady-state volume of distribution (V_{ss}). In case of discrepancies between the predicted V_{ss} and observed value (0.6683 L/kg based on meta-analysis of literature data), adjustments were made to the K_p scalar (scalar allowing for the uniform scaling of all predicted K_p values) to match the observed V_{ss} value. The average total body clearance of metronidazole in healthy adults was 4.28 L/h based on meta-analysis of literature data.[17,19,20,22–27,34,35] The intrinsic clearances of hepatic enzymes, including CYP2A6, CYP2E1, and UGT1A9, were calculated using the retrograde tool in Simcyp, considering their respective contributions to hepatic clearance (Table 3). The renal clearance was 0.2568 L/h, representing 6% of the total clearance. This value served as an input parameter for renal elimination when the Mech-Kim model was not activated (Adult Model I). However, upon activating the Mech-Kim model (Adult Model II), the intrinsic CL_{PD} (mL/min/million cells), which described tubular reabsorption, was optimized to align the predicted renal clearance with the observed value (Table 3).

The adult PBPK model was verified with the clinical observations of metronidazole under different doses (Table S2). Population simulations using 10 trials with 10 subjects in each trial were performed using the Sim-Healthy Volunteers module. In each simulation, dosing regimens, age, gender ratios, and other study elements were aligned with respective study characteristics. The model's predictive performance was considered good when average or individual observed concentrations fell within the 90% confidence interval of the predicted curve. Additionally, the two-fold range criterion was used for average concentrations and mean pharmacokinetic parameters (clearance and peak concentration (C_{max})). The mean relative deviation (MRD) and average fold error (AFE) were computed to assess the accuracy and bias of the model predictions.[36] Predictions with an MRD and AFE of ≤2 were considered reasonable.

TABLE 3 Input data and model parameters for final metronidazole PBPK model in adults.

Parameter	Model input value	Sources/comments
Physicochemical data and plasma binding		
Molecular weight (g/mol)	171.16	PubChem
$\log P$	−0.02	Davis et al.[32]
Compound type	Monoprotic Base	DrugBank
pK_a	2.49	Shalaeva et al.[33]
Fraction unbound in plasma	0.9	Mamada et al.[31]
Blood/plasma concentration ratio	1.07	Mamada et al.[31]
Plasma binding component	Albumin	
Distribution		
Distribution model	Full PBPK model	
Volume of distribution at steady state (V_{ss}, L/kg)	0.6629	Predicted via Rodgers and Rowland method with a K_p scalar of 1.35
Elimination		
CYP2A6 mediated CL_{int} (Liver) (µL/min/pmol)	0.0361	Calculated via retrograde model in Simcyp
CYP2E1 mediated CL_{int} (Liver) (µL/min/pmol)	0.0059	Calculated via retrograde model in Simcyp
UGT1A9 mediated CL_{int} (Liver) (µL/min/pmol)	0.0045	Calculated via retrograde model in Simcyp
CL_R (L/h)[a]	0.2568	Meta-analysis based on data in literature
CL_{PD} (mL/min/million proximal tubular cells)[b]	0.125	Manually optimized to match the observed renal clearance in adults (0.2568 L/h)

[a]Input value of the adult renal clearance for Adult Model I.

[b]Intrinsic passive diffusion clearance of tubular reabsorption for Adult Model II.

Scaling adult PBPK model to pediatrics

The validated adult PBPK models (Adult Model I and Adult Model II) were scaled to pediatrics (Pediatric Model I and Pediatric Model II) using the Sim-Pediatric module in Simcyp, which incorporated age-related changes in anatomical and physiological parameters. For Pediatric Model I, renal clearance was calculated using Equation 4 based on the predicted GFR by the Johnson model. For Pediatric Model II, the Mech-Kim model was utilized to predict the renal clearance. The built-in ontogeny profiles of the metabolic enzymes CYP2A6, CYP2E1, and UGT1A9 versus age (years) were utilized (Equations 6–8) to describe the developmental hepatic metabolism of metronidazole in both pediatric models. The same principles of simulations and verification criteria as the adult PBPK model were adopted in the validation of the pediatric PBPK model.

$$\text{Fraction of adult CYP2A6 activity} = \frac{\text{Age}^{5.68}}{0.21^{5.68} + \text{Age}^{5.68}} \tag{6}$$

$$\text{Fraction of adult CYP2E1 activity} = \frac{0.99 \cdot \text{Age}^{0.5}}{0.23^{0.5} + \text{Age}^{0.5}} \tag{7}$$

$$\text{Fraction of adult UGT1A9 activity} = 0.0541 + \frac{(1.012 - 0.0541) \cdot \text{Age}^{5.771}}{0.07228^{5.771} + \text{Age}^{5.771}} \tag{8}$$

RESULTS

Predicted pediatric renal clearance by empirical and mechanistic approaches

The renal clearances predicted by the different empirical and mechanistic models are presented in Tables S4–S6, while the calculated ratios of renal clearance are shown in Figure 1 and Figure S2. Simulation analysis demonstrated that as the F_{reabs} of a drug in adults increased, the ratio of renal clearance predicted by the Mech-KiM model to those predicted by the GFR-based models (Johnson model and Rhodin model) showed an increased difference in children under 2 years old (Figure 1 and Figure S2). When utilizing a drug with a f_u value of 0.9 (Figure 1, panel a): (1) if the F_{reabs} of the drug was ≤70%, the ratios of predicted renal clearance using both the Mech-KiM model and the Johnson model throughout childhood were consistently within a two-fold error range; (2) If the F_{reabs} of the drug was 80%, the ratios of predicted renal clearance exceeded the two-fold error range in children younger than 1 month, with ratios ranging from 2.0 (at 1 month) to 2.6 (at 1 day); (3) If the F_{reabs} of the drug was 90%, the ratios of predicted

renal clearance exceeded the twofold error range in children younger than 6 months, with ratios ranging from 2.0 (at 6 months) to 4.5 (at 1 day); (4) If the F_{reabs} of the drug was 95%, the ratios of predicted renal clearance exceeded the two-fold error range in children younger than 2 years, with ratios ranging from 2.2 (at 2 years) to 8.3 (at 1 day).

Changes in the drug's f_u to lower values (e.g., 0.5 and 0.1) did not notably affect the trend of predicted renal clearance ratios across ages (Figure 1, panel b and panel c). The trend of ratios of predicted renal clearance using the Mech-KiM model and the Rhodin model (Figure S2) was not significantly different from those using the Mech-KiM model and the Johnson model.

Using the empirical GFR scaling models, the calculated F_{reabs} of the hypothetical drug in children mostly remained consistent with adult levels when f_u was 0.9 (Figure S3, panels a and d). When f_u was changed to 0.5 (panels b and e) or 0.1 (panels c and f), and the drug's F_{reabs} in adults was ≤50%, the predicted F_{reabs} in children gradually showed a slight increase as age decreased. In contrast, with the Mech-KiM model, the predicted F_{reabs} in children gradually decreased as age decreased (Figure S3, panels g–i). Changes in f_u values did not significantly affect the trends of F_{reabs} in childhood for different models.

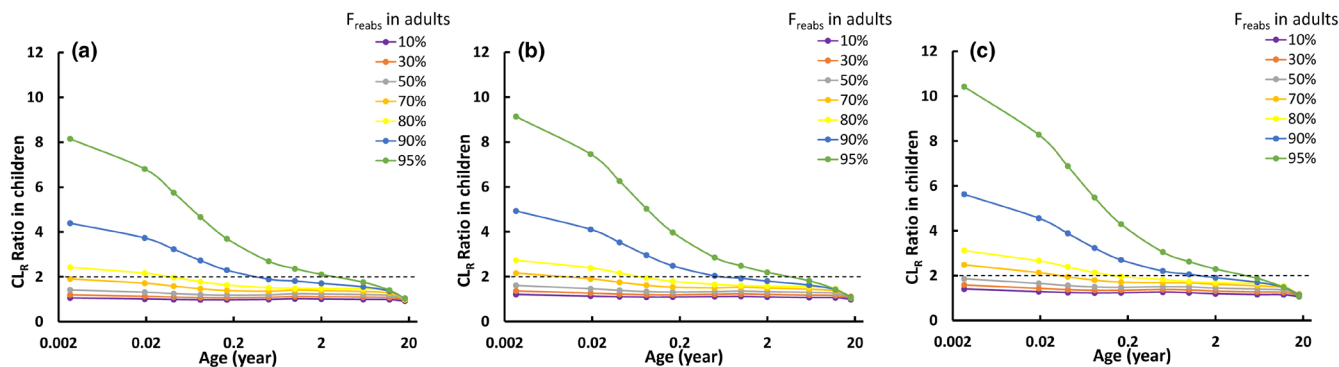Figure 2 showed the maturation profiles of GFR (based on the Johnson and Rhodin models) and CL_{PD} (based on the Mech-KiM model) in children relative to adult levels. The data indicated that glomerular filtration matured more rapidly than passive tubular reabsorption. Additionally, the maturation profile of CL_{PD} was not influenced by the adult F_{reabs} and f_u of the hypothetical drug (data not shown).

For the hypothetical drug with both renal and hepatic elimination, the ratios of renal clearance predicted by the Mech-Kim model to total clearance in children at various ages are shown in Figure S4. When the ratio of renal to total clearance was 0.9 in adults, the predicted ratios throughout childhood remained largely unchanged, regardless of the variations in predefined F_{reabs} in adults. However, when the ratio of renal to total clearance was 0.5 or 0.1 in adults, the predicted ratios decreased when adult F_{reabs} was less than 80%, and increased when adult F_{reabs} exceeded 90%.

### Pediatric PBPK modeling of metronidazole

Adult PBPK model

The initial predicted V_{ss} (0.5107 L/kg) for metronidazole, based on its physicochemical data (Table 3), was notably

FIGURE 1 The ratio of renal clearance predicted by the Mech-KiM model to those predicted by the GFR-based scaling model (Johnson model) in children of different ages. Panel (a): Virtual drug in adults with a f_u of 0.9; panel (b): Virtual drug in adults with a f_u of 0.5; panel (c): Virtual drug in adults with a f_u of 0.1.

FIGURE 2 Maturation profiles of glomerular filtration rate (GFR) and bidirectional passive diffusion clearance (CL_{PD}) for tubular reabsorption in children relative to adult levels. GFR was predcited based on the Johnson and Rhodin models, and CL_{PD} was predicted by the Mech-KiM model.
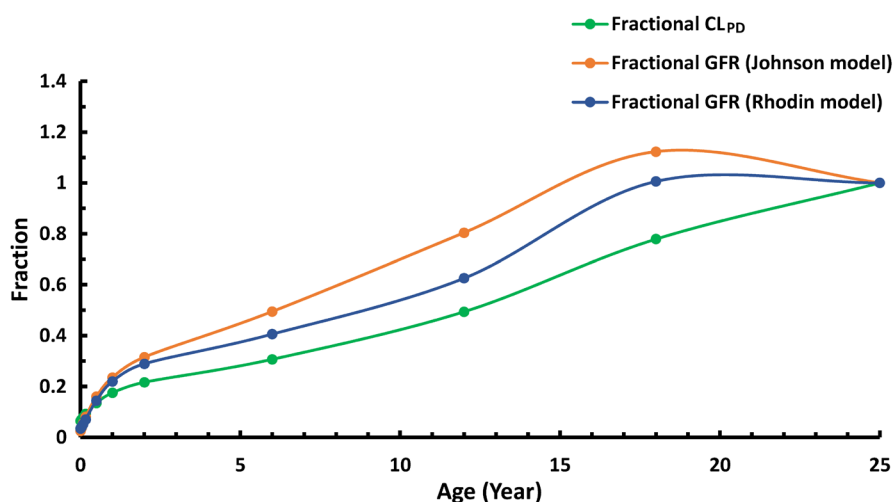

lower than the observed value (0.6683 L/kg) for both Adult Model I and Model II. To correct this discrepancy, an optimized K_p scalar of 1.35 was applied, aligning the predicted V_{ss} with the observed value. After this adjustment, both models effectively described the concentration-time curves for various intravenous doses (0.4 g–2.0 g) of metronidazole, with most observations falling within the 90% prediction interval of the simulated data (Figure S5). As there were no significant differences in predictions between Adult Model I and Model II, only the results of Adult Model II are presented. Out of a total of 147 data points, only 11 (7.5%) of the observed data points deviated by more than two-fold from the average predicted values (Figure S6), indicating no significant prediction bias by the model. Additionally, key pharmacokinetic parameters such as CL and C_{max} had average observed values within 2-fold of the predicted range (Table S7). Furthermore, the calculated mean MRD was 1.06 (range: 1.01–1.15), and the mean AFE was 1.13 (range: 1.01–1.37). These results demonstrated that the adult PBPK model accurately discribled the pharmacokinetic characteristics of metronidazole in adult subjects. A representative metronidazole

Simcyp workspace of the Fredricsson et al. study[25] for the Adult Model II is provided as the supplement.

Pediatric PBPK model

Pediatric Model I and Model II were evaluated based on mean and individual observed plasma concentration-time data as surrogates for renal clearance (in the absence of observed renal clearance data) from single or multiple doses of metronidazole studies in pediatric populations (0 day < PNA < 10 months). The predictions for both pediatric models were very consistent with observed mean concentration data in Rubenson et al.'s study of children aged 3.5–10 months (Figure 3, panel a and panel b).[30] However, in Jager et al.'s study of neonates aged 1–2 days,[28] Pediatric Model I overestimated mean drug concentrations during the elimination phase (Figure 3, panel c). In contrast, Pediatric Model II's predictions were well-aligned with the observed values for the same group, showing an MRD of 1.01 and an AFE of 1.18 (Figure 3, panel d). In this neonate group, the predicted
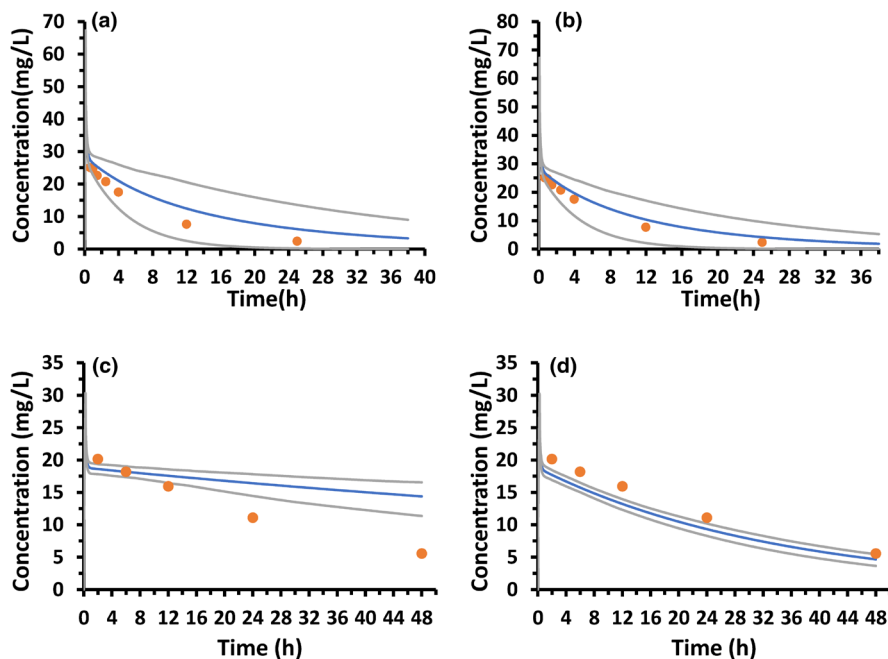
FIGURE 3 Observed versus predicted plasma concentration-time profiles based on Pediatric Model I (panels a, c) and Pediatric Model II (panels b, d) for Rubenson et al. (panels a, b) and Jager et al. (panels c, d) studies. The orange dots represent the mean observations. The blue and gray lines represent the predicted mean and the 90% prediction interval of simulated plasma concentration-time profiles by Pediatric Model I and Pediatric Model II.
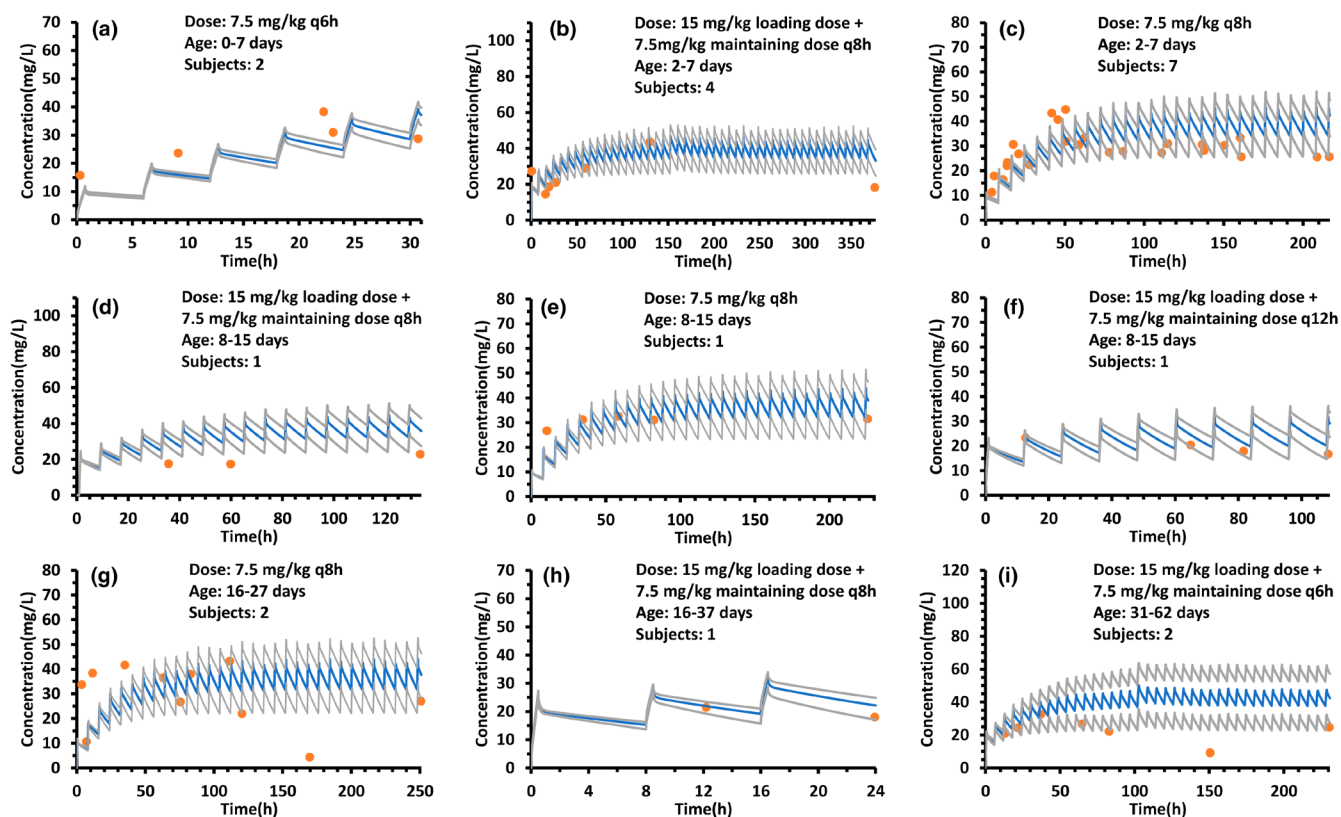
FIGURE 4 Observed versus predicted plasma concentration-time profiles by Pediatric Model II of metronidazole in pediatrics following different intravenous dosing regimens of metronidazole in Cohen et al. study. The orange dots represent individual-level observations. The blue and gray lines represent the predicted mean and 90% prediction interval of simulated plasma concentration-time profiles by Pediatric Model I. Literature data sources are presented in Table S3.

renal clearance and total clearance by Pediatric Model I were 0.0067 and 0.0148 L/h, respectively, while those by Pediatric Model II were 0.065 and 0.073 L/h, respectively. The predicted renal clearance and total clearance of metronidazole by Pediatric Model II were 9.70 times and 4.93 times higher than those predicted by Pediatric Model I. The superior predictive performance of Pediatric Model II (Figure 4), compared to Pediatric Model I (Figure S7), was

further validated by individual observed concentrations in pediatric subjects with a PNA ≤60 days.[29]

DISCUSSION

In this study, the adequacy of empiric GFR-based scaling methods was investigated for predicting pediatric renal clearance of hypothetical drugs with varying degrees of tubular reabsorption, using the mechanistic Mech-KiM model as a reference. A PBPK model of metronidazole, spanning from full-term neonates to adults, was constructed to evaluate the predictive performance of renal clearance extrapolation across different ages of children using these methods.

Hypothetical drugs with various f_u and F_{reabs} characteristics were used to systematically investigate the differences between GFR-based scaling methods and the Mech-KiM model in predicting pediatric renal clearance. Our results indicated that when F_{reabs} is ≤70%, the differences between the GFR-based scaling methods and the Mech-KiM model in predicted pediatric renal clearance are generally within a twofold range throughout childhood. In such cases, the empirical GFR-based scaling methods seem adequate for extrapolating pediatric renal clearance without the need to use the Mech-KiM model. However, for drugs with strong tubular reabsorption (e.g., $F_{reabs} > 70\%$), the GFR-based scaling methods showed greater than twofold differences compared to the Mech-KiM model in predicting renal clearance for young children (e.g., children under 1 month when F_{reabs} is 80%, and children under 2 years when F_{reabs} is 95%).

To validate which method, the GFR-based scaling methods or the Mech-KiM model, more accurately predicts pediatric renal clearance, we selected metronidazole, a model drug with a renal reabsorption of 96%. Due to the lack of observed renal clearance data for metronidazole in children, a direct comparison of predicted and observed renal clearances was not possible. Therefore, using observed pediatric plasma concentrations of metronidazole, we evaluated the predictive performance of PBPK models employing either the GFR-based scaling methods or the Mech-KiM model in forecasting pediatric concentrations. As a primarily cleared via hepatic metabolism drug in adults, metabolism fraction of CYP2E1 and UGT1A9 for metronidazole is well-defined.[17,18] Although both CYP2A6 and CYP3A4 are involved in the formation of its major metabolite, 2-hydroxymetronidazole, which accounts for 62% of the administered dose, in vitro metabolism studies have shown that 96% of 2-hydroxymetronidazole formation is attributed to CYP2A6.[37] Given that CYP2A6 is the primary enzyme responsible for the 2-hydroxylation of metronidazole, we assumed that the formation of

2-hydroxymetronidazole was entirely catalyzed by CYP2A6 during PBPK model development. With this assumption, Pediatric Model I ulitizing GFR-based scaling method for renal clearance prediction overestimated mean drug concentrations during the elimination phase in Jager et al.'s study of neonates aged 1 to 2 days.[28] Further sensitivity analysis was conducted by testing an unlikely scenario, assuming 31% of metronidazole is metabolized via CYP2A6 and 31% via CYP3A4 in adults. The resulting pediatric PBPK Model I still significantly overestimated the metronidazole concentrations in neonates (Figure S8). Instead, switching to Pediatric Model II utilizing the Mech-KiM model for predicting renal clearance yielded predictions closely aligned with the observed concentrations for the same group. This indicates that accurate prediction of metronidazole renal clearance by the Mech-KiM model is crucial for total clearance in neonates, surpassing the importance of hepatic clearance. In this neonate group, Pediatric Model II predicts that 89% of the total clearance of metronidazole is attributed to renal clearance. This finding is supported by previous studies, which indicate that metronidazole undergoes minimal metabolism (about 10%) in neonates due to the low activity of CYP2A6,[38] with renal excretion being the predominant factor influencing its elimination.[28] Figure S9 illustrates the changes in the simulated fraction metabolized and fraction excreted for metronidazole from birth to adulthood, highlighting the dynamic shifts in the relative contributions of hepatic metabolism and renal excretion pathways. As depicted, drugs like metronidazole that undergo extensive reabsorption typically have low fractional CL_R in adults. A mechanistic understanding of renal excretion for such drugs is often of low importance in adults but can be crucial for accurate PK predictions in children, particularly in neonates.

The GFR-based scaling methods do not account for the maturation of the tubular reabsorption process. As a result, the predicted fraction of tubular reabsorption in children remains nearly identical to or slightly higher than adult levels (due to age-dependent changes in pediatric f_u). This might potentially lead to underestimated renal clearance in children and consequently overestimated drug concentrations. In contrast, the Mech-KiM model describes the age-related anatomy and physiology of the kidney in a mechanistic manner. The maturation of the reabsorption process is linked to the growth of kidney weight (Equation 5), resulting in decreased tubular reabsorption as children age decreases. The slower maturation of passive tubular reabsorption compared to glomerular filtration aligns well with previous knowledge of glomerulo-tubular imbalance.[11] Nevertheless, linking CL_{PD} to tubular surface area appears to be a more mechanistic approach than linking it to kidney weight, as

demonstrated in a recently reported mechanistic kidney model incorpating 35 compartments.[39]

Notably, the overall drug clearance in children at different ages depends on the dynamic contributions of renal excretion and hepatic metabolism. The potential inaccuracies in predicting renal clearance for extensively tubular reabsorbed drugs by GFR-based scaling methods may not significantly affect the prediction of total clearance. In this study, we explored the impact of renal clearance, as predicted by the Mech-KiM model, on overall drug clearance in pediatric populations by assuming a hypothetical drug with varying ratios of renal to total clearance in adults. Under the assumption of no ontogeny for hepatic clearance, we found that the ratios of renal to total clearance in childhood changed significantly when the renal clearance ratio in adults was moderate (e.g., 0.5). However, this simplified scenario does not capture the complexity of real-world conditions, as hepatic metabolism mediated by CYP enzymes (e.g., CYP3A4 and CYP2A6) follows distinct ontogeny patterns.

In conclusion, our study demonstrated that the GFR-based scaling methods could be adequate for predicting pediatric renal clearance for drugs with a tubular reabsorption rate of ≤70%, whereas the Mech-KiM model might be considered for drugs with a tubular reabsorption rate of >70%.

AUTHOR CONTRIBUTIONS

S.L., X.Y., Q.W., Z.C., F.L., and F.X. wrote the manuscript. F.X. designed the research. S.L. and X.Y. performed the research. Q.W., S.L., X.Y., and F.X. analyzed the data.

CONFLICT OF INTEREST STATEMENT

All authors declared no competing interests for this work.

ORCID

Sanwang Li https://orcid.org/0000-0001-5979-5133
Xuexin Ye https://orcid.org/0009-0006-2945-5879
Qiushi Wang https://orcid.org/0009-0006-8764-2031
Zeneng Cheng https://orcid.org/0000-0001-9352-9744
Feiyan Liu https://orcid.org/0000-0002-3711-2810
Feifan Xie https://orcid.org/0000-0002-9038-2676

REFERENCES

1. Chase SL, Sutton JD. Lisinopril: a new angiotensin-converting enzyme inhibitor. *Pharmacotherapy*. 1989;9:120-128; discussion 128–130.
2. Li S, Xie F. Foetal and neonatal exposure prediction and dosing evaluation for ampicillin using a physiologically-based pharmacokinetic modelling approach. *Br J Clin Pharmacol*. 2023;89:1402-1412.
3. Shen DD, Azarnoff DL. Clinical pharmacokinetics of methotrexate. *Clin Pharmacokinet*. 1978;3:1-13.
4. Talevi A, Bellera CL. Renal drug excretion. *The ADME Encyclopedia: A Comprehensive Guide on Biopharmacy and Pharmacokinetics*. Springer International Publishing; 2021.
5. Fagerholm U. Prediction of human pharmacokinetics – renal metabolic and excretion clearance. *J Pharm Pharmacol*. 2007;59:1463-1471.
6. Scotcher D, Jones C, Rostami-Hodjegan A, Galetin A. Novel minimal physiologically-based model for the prediction of passive tubular reabsorption and renal excretion clearance. *Eur J Pharm Sci*. 2016;94:59-71.
7. Lin W, Yan J-H, Heimbach T, He H. Pediatric physiologically based pharmacokinetic model development: current status and challenges. *Curr Pharmacol Rep*. 2018;4:491-501.
8. Wang K, Jiang K, Wei X, Li Y, Wang T, Song Y. Physiologically based pharmacokinetic models are effective support for pediatric drug development. *AAPS PharmSciTech*. 2021;22:208.
9. Johnson TN, Rostami-Hodjegan A, Tucker GT. Prediction of the clearance of eleven drugs and associated variability in neonates, infants and children. *Clin Pharmacokinet*. 2006;45:931-956.
10. Rhodin MM, Anderson BJ, Peters AM, et al. Human renal function maturation: a quantitative description using weight and postmenstrual age. *Pediatr Nephrol*. 2009;24:67-76.
11. Zhang Y, Mehta N, Muhari-Stark E, Burckart GJ, van den Anker J, Wang J. Pediatric renal ontogeny and applications in drug development. *J Clin Pharmacol*. 2019;59(Suppl 1):S9-s20.
12. Salem F, Johnson TN, Hodgkinson ABJ, Ogungbenro K, Rostami-Hodjegan A. Does "birth" as an event impact maturation trajectory of renal clearance via glomerular filtration? Reexamining data in preterm and full-term neonates by avoiding the creatinine bias. *J Clin Pharmacol*. 2021;61:159-171.
13. Salem F, Small BG, Johnson TN. Development and application of a pediatric mechanistic kidney model. *CPT Pharmacometrics Syst Pharmacol*. 2022;11:854-866.
14. Cheung KWK, van Groen BD, Spaans E, et al. A comprehensive analysis of ontogeny of renal drug transporters: mRNA analyses, quantitative proteomics, and localization. *Clin Pharmacol Ther*. 2019;106:1083-1092.
15. Maharaj AR, Edginton AN. Physiologically based pharmacokinetic modeling and simulation in pediatric drug development. *CPT Pharmacometrics Syst Pharmacol*. 2014;3:e150.
16. Neuhoff S, Gaohua L, Burt H, et al. Accounting for transporters in renal clearance: towards a mechanistic kidney model (mech KiM). In: Sugiyama Y, Steffansen B, eds. *Transporters in Drug Development: Discovery, Optimization, Clinical Study and Regulation*. Springer New York; 2013.

17. Jensen JC, Gugler R. Single- and multiple-dose metronidazole kinetics. *Clin Pharmacol Ther*. 1983;34:481-487.

18. Gao R, Li L, Xie C, Diao X, Zhong D, Chen X. Metabolism and pharmacokinetics of morinidazole in humans: identification of diastereoisomeric morpholine N+-glucuronides catalyzed by UDP glucuronosyltransferase 1A9. *Drug Metab Dispos*. 2012;40:556-567.

19. Houghton GW, Smith J, Thorne PS, Templeton R. The pharmacokinetics of oral and intravenous metronidazole in man. *J Antimicrob Chemother*. 1979;5:621-623.

20. Sprandel KA, Schriever CA, Pendland SL, et al. Pharmacokinetics and pharmacodynamics of intravenous levofloxacin at 750 milligrams and various doses of metronidazole in healthy adult subjects. *Antimicrob Agents Chemother*. 2004;48:4597-4605.

21. Mattila J, Männistö PT, Mäntylä R, Nykänen S, Lamminsivu U. Comparative pharmacokinetics of metronidazole and tinidazole as influenced by administration route. *Antimicrob Agents Chemother*. 1983;23:721-725.

22. Loft S, Døssing M, Poulsen HE, et al. Influence of dose and route of administration on disposition of metronidazole and its major metabolites. *Eur J Clin Pharmacol*. 1986;30:467-473.

23. Jessa MJ, Goddard AF, Barrett DA, Shaw PN, Spiller RC. The effect of omeprazole on the pharmacokinetics of metronidazole and hydroxymetronidazole in human plasma, saliva and gastric juice. *Br J Clin Pharmacol*. 1997;44:245-253.

24. Houghton GW, Thorne PS, Smith J, Templeton R, Collier J. Comparison of the pharmacokinetics of metronidazole in healthy female volunteers following either a single oral or intravenous dose. *Br J Clin Pharmacol*. 1979;8:337-341.

25. Fredricsson B, Hagström B, Nord CE, Rane A. Systemic concentrations of metronidazole and its main metabolites after intravenous oral and vaginal administration. *Gynecol Obstet Invest*. 1987;24:200-207.

26. Das S, Li J, Armstrong J, Learoyd M, Edeki T. Randomized pharmacokinetic and drug-drug interaction studies of ceftazidime, avibactam, and metronidazole in healthy subjects. *Pharmacol Res Perspect*. 2015;3:e00172.

27. Bergan T, Thorsteinsson SB. Pharmacokinetics of metronidazole and its metabolites in reduced renal function. *Chemotherapy*. 1986;32:305-318.

28. Jager-Roman E, Doyle PE, Baird-Lambert J, Cvejic M, Buchanan N. Pharmacokinetics and tissue distribution of metronidazole in the new born infant. *J Pediatr*. 1982;100:651-654.

29. Cohen-Wolkowiez M. *Antibiotic Safety in Infants with Complicated Intra-Abdominal Infections - Metronidazole (Version 1) [Dataset]*. NICHD Data and Specimen Hub; 2023.

30. Rubenson A, Rosetzky A. Single dose prophylaxis with metronidazole in infants during abdominal surgery: a pharmacokinetic study. *Eur J Clin Pharmacol*. 1986;29:625-628.

31. Mamada H, Iwamoto K, Nomura Y, Uesawa Y. Predicting blood-to-plasma concentration ratios of drugs from chemical structures and volumes of distribution in humans. *Mol Divers*. 2021;25:1261-1270.

32. Davis JL, Little D, Blikslager AT, Papich MG. Mucosal permeability of water-soluble drugs in the equine jejunum: a preliminary investigation. *J Vet Pharmacol Ther*. 2006;29:379-385.

33. Shalaeva M, Kenseth J, Lombardo F, Bastin A. Measurement of dissociation constants (pKa values) of organic compounds by multiplexed capillary electrophoresis using aqueous and cosolvent buffers. *J Pharm Sci*. 2008;97:2581-2606.

34. Mattie H, Dijkmans BA, van Gulpen C. The pharmacokinetics of metronidazole and tinidazole in patients with mixed aerobic–anaerobic infections. *J Antimicrob Chemother*. 1982;10 Suppl A:59-64.

35. Muscará MN, Pedrazzoli J, Miranda EL, et al. Plasma hydroxy-metronidazole/metronidazole ratio in patients with liver disease and in healthy volunteers. *Br J Clin Pharmacol*. 1995;40:477-480.

36. Edginton AN, Schmitt W, Willmann S. Development and evaluation of a generic physiologically based pharmacokinetic model for children. *Clin Pharmacokinet*. 2006;45:1013-1034.

37. Pearce RE, Cohen-Wolkowiez M, Sampson MR, Kearns GL. The role of human cytochrome P450 enzymes in the formation of 2-hydroxymetronidazole: CYP2A6 is the high affinity (low km) catalyst. *Drug Metab Dispos*. 2013;41:1686-1694.

38. Wang LA, Gonzalez D, Leeder JS, et al. Metronidazole metabolism in neonates and the interplay between ontogeny and genetic variation. *J Clin Pharmacol*. 2017;57:230-234.

39. Huang W, Isoherranen N. Development of a dynamic physiologically based mechanistic kidney model to predict renal clearance. *CPT Pharmacometrics Syst Pharmacol*. 2018;7:593-602.

SUPPORTING INFORMATION

Additional supporting information can be found online in the Supporting Information section at the end of this article.